Observer Based Controller for Internal Combustion Engine

Marco Meza-Aguilar*, Juan Diego Sánchez-Torres*, Alexander Loukianov*, Antonio Navarrete-Guzmán* and Jorge Rivera†
*Department of Electrical Engineering, CINVESTAV Unit Guadalajara, Zapopan, Jalisco, México 45019
Email:ameza@gdl.cinvestav.mx, dsanchez@gdl.cinvestav.mx, louk@gdl.cinvestav.mx, anavarret@gdl.cinvestav.mx
†Department of Electrica Engineering, DIVEC CUCEI University of Guadalajara, Guadalajara, Jalisco, México 44430
Email: jorge.rivera@cucei.udg.mx

***Abstract*—In this work, an observer-based controller for an internal combustion engine is presented. At first, an algorithm for the estimation of an unknown function of the internal combustion engine is designed, since it is very difficult to obtain direct measurements of this variable. This estimator is based on sliding mode algorithms, providing a finite time and robust estimation, using only measurements from the velocity of the engine. On the other hand, with the measured velocity and the estimates of the other variables, a robust controller is synthesized for the engine. In order to considerate the actuator dynamics, the proposed control scheme is based on the master-slave structure, regarding the controller for the actuator as the slave one. For this scheme, the backstepping algorithm is used to design the master controller. Then, the calculated control input signal to the engine is used as a reference for the throttle actuator which is driven by a direct current (DC) motor. Thus, a high-order sliding mode controller is applied to the actuator in order to track the control input signal and reject perturbations, as the applied mechanical load, regulating the velocity of the combustion engine. Numerical simulations show the efficient performance of this proposal.**

I. Introduction

The automotive industry is constantly pursuing to satisfy the end-user demand of fuel efficient engines along with free running of the vehicle, almost every modern car is equipped with on-board diagnostic softwares in their electronic control units (ECUs) to control and monitor the engine operations.

Therefore several researchers are focused in solving problems related to the design of the feedback controller in the major subsystem of a vehicle that enables further improvement via application of modern speed control strategies is a combustion engine with an electrically driven throttle.

The engine speed control problem has been considered in several publications [1], [2], [3], [4]. Usually, these controllers are based on mean value engine models (MVEMs) [5] because it can describe the behavior of spark ignition (SI) engines [6], [7]. The MVEMs models describe the time development of the most important measurable engine variables on time scales a little larger than an engine cycle [8],[9] . The states of an SI engine are usually the fuel film flow or mass, the crank shaft speed and the manifold pressure, each described with a differential equation driven by a control input: these are the injected fuel flow, the spark advance and the throttle angle respectively.

In this work, it is presented a novel approach to the trajectory tracking for then engine velocity driven by a electronic throttle. This proposal is based on the backstepping technique [10], combined with high-order sliding modes (HOSM) algorithms [11]. The SM methods are applied with the idea to drive the dynamics of a system to a sliding manifold, which is an integral manifold with finite reaching time [12], on which the closed-loop system motion has desired properties as the finite time stability and robustness in presence of parameter variations and external disturbances [13].

Taking advantage of those features, an estimator for an unknown function of the internal combustion engine and the pressure in the intake manifold is designed. This design uses the equivalent control [13] method for observers as is shown in [14], [15]. Instead the use of relay stabilizing terms, the so-called *generalized super-twisting* [16] (based on the *super-twisting* algorithm [17]) is applied to drive the estimation error to zero as proposed by [18].

With the estimates provided by the proposed observer we apply a backstepping control technique to track a velocity reference for the engine. Then, the calculated control input signal to the engine is used as a reference signal for the actuator, that is controlled by using an HOSM controller. The HOSM algorithm is applied to the actuator in order that can track the control input signal, finally regulating the throttle position of the combustion engine.

II. Mean Value Engine Models

In this section the mathematical model of the Mean Value Engine Model (MVEM) of Spark Ignition (SI) is presented [19].

A. The Crank Shaft Speed State Equation

The crank shaft state equation is derived using straight forward energy conservation considerations. Energy is inserted into the crank shaft via the fuel flow. In order to avoid modeling the cooling and exhaust system losses, the thermal efficiency of the engine is inserted as a multiplier of the fuel mass flow. Losses in pumping and friction dissipate rotational energy while some of the energy goes into the load. Physically this is expressed as a conservation law: the rate of a change of the crank shaft rotational kinetic energy is equal to sum of the power available to accelerate the crank shaft and that of the load:

$$\dot{n}_e = -\frac{(P_f + P_p + P_b)}{J_e n_e} + \frac{H_u \eta_i \dot{m}_f}{J_e n_e} \tag{1}$$

where n_e is the crank shaft speed, J_e is the moment of inertia in the rotating parts of the engine, P_f, P_p and P_b are the power lost to the friction, pumping losses and the load, respectively, H_u is the fuel burn value, η_i is the thermal efficiency, and $\dot{m}_f$ is the fuel mass flow.
The loss functions P_f and P_p form the load input to the engine and can be implemented to match a desired operating scenario. They are usually regressions based on data from engine measurements and can be modeled by the following regressions functions:

$$\begin{aligned} P_f =& 0.0135n_e^3 + 0.2720n_e^2 + 1.6730n_e \\ P_p =& n_e P_m(0.2060n_e - 0.9690). \end{aligned} \tag{2}$$

where P_m is the pressure in the intake manifold. It has been found convenient to express the load power as the function:

$$P_b = k_b n^3 \tag{3}$$

where k_b is the loading parameter. It is ajusted in such a way than the engine is loaded to the desired power or torque level at a given operating point.

The thermal efficiency η_i is also a regression and can be modeled by the following polynomial:

$$\eta_i = 0.55(1 - 0.39{n_e}^{-0.36})(0.82 + 0.58P_m - 0.39{P_m}^2). \tag{4}$$

B. The Fuel Mass Flow Rate

The fuel mass flow rate $\dot{m}_f$ is typically determined by a fuel injection control system which attempts to maintain a stoichiometric air fuel ratio. It is assumed this ratio is successfully maintained in the cylinder. Thus, the fuel mass flow rate $\dot{m}_f$ is related to the outflow from the intake manifold into the cylinders of the engine as follows [9]:

$$\dot{m}_f = \frac{\dot{m}_{ao}}{\lambda L_{th}} \tag{5}$$

where $\dot{m}_{ao}$ is the air mass flow rate out of the intake manifold and into the cylinder, L_{th} is the stoichiometric air/fuel mass ratio for the Fuel and λ is the air/fuel equivalence ratio.

The third-level of heading follows the style of the second-level heading.

C. Manifold Pressure State Equation

In the derivation of the manifold pressure state equation, the common procedure is to use the conservation of air mass in the intake manifold:

$$\dot{m}_m = \dot{m}_{ai} - \dot{m}_{ao} \tag{6}$$

where $\dot{m}_m$ is the air mass flow in the intake manifold, $\dot{m}_{ai}$ and $\dot{m}_{ao}$ represent mass flow rate in and out of the intake manifold, i.e. through the throttle valve and into the cylinder, respectively.

The pressure in the intake manifold P_m can be related to the air mass in the manifold m_m using the ideal gas equation

$$P_m V_m = m_m R T_m \tag{7}$$

where R is the ideal gas constant, T_m is the intake manifold temperature and V_m is the intake manifold volume.

Taking time derivatives of (7) and using (6), the intake manifold pressure equation is obtained of the form

$$\dot{P}_m = \frac{RT_m}{V_m}(\dot{m}_{ai} - \dot{m}_{ao}). \tag{8}$$

The expressions forms of $\dot{m}_{ai}$ and $\dot{m}_{ao}$ are described in the following Subsections.

1) Port Air Mass Flow: The air mass flow $\dot{m}_{ao}$ at the intake port of the engine can be obtained from the speed-density equation [19] as

$$\dot{m}_{ao} = \sqrt{\frac{T_m}{T_a}}\frac{V_d}{120RT_m}(e_v P_m)n_e. \tag{9}$$

On the other hand, the relation between P_m and the speed n_e is given by [19]

$$e_v P_m = s_i P_m - y_i \tag{10}$$

where T_a is the ambient temperature, V_d is the engine displacement, the manifold pressure slope s_i is slightly less than 1 and the manifold pressure intercept y_i is close to 0.10; they are always positive and depend mostly on the crank shaft speed. Moreover, they should not change much over the range operating an engine from one engine to another except for those which are highly tuned. The form of equation (10) has been known phenomenologically at Ford for many years but in [19] this equation has been derived from physical considerations. This means that it can be rapidly applied to many different engines with basically only a knowledge of a few physical constants, and this is the advantage of the derivation above.

Using now (10) the speed-density equation (9) becomes

$$\dot{m}_{ao} = \sqrt{\frac{T_m}{T_a}}\frac{V_d}{120RT_m}(s_i P_m + y_i)n_e. \tag{11}$$

2) Throttle Air Mass Flow: The second important equation is the manifold pressure state equation, which is used to describe the air mass flow past the throttle plate. This part of the model based on the isoentropic flow equation for a converging-diverging nozzle, is given by [19]

$$\dot{m}_{ai} = \dot{m}_{ai1}\frac{P_a}{\sqrt{T_m}}\beta_1(\alpha)\beta_2(P_r) + \dot{m}_{ai0} \tag{12}$$

where P_a is the ambient pressure, $\dot{m}_{ai1}$ and $\dot{m}_{ai0}$ are constants, α is the throttle angle and $\beta_1(\alpha)$ is the throttle plate angle dependency which can be described by the following function as an approximation to the normalized open area:

$$\beta_1(\alpha) = 1 - cos(\alpha) - \frac{{\alpha_0}^2}{2} \tag{13}$$

where α_0 is the fully closed throttle plate angle (radians). The function $\beta_1(\alpha)$ serves as the function of an area dependent on the discharge coefficient $\beta_2(P_r)$, and it is defined by the isentropic flow expression:

$$\beta_2(P_r) = \begin{cases} 1 & P_r < P_c \\ \sqrt{1 - \left(\frac{P_r - P_c}{1 - P_c}\right)} & P_c \leq P_r \end{cases} \tag{14}$$

where $P_r = P_m/P_a$, and $P_c = 0.4125$ is the critical pressure (turbulent flow).

D. Internal Combustion Engine Model

Using (1-14), the MVEMs state system is obtained of the following form:

$$\begin{aligned} \dot{n_e} &= -f_1(n_e, P_m) + b_1(n_e, P_m) \\ \dot{P_m} &= \frac{RT_m}{V_m}\left(f_2(n, P_m) + b_2(P_m)\beta_1(\alpha)\right) \end{aligned} \tag{15}$$

where
$f_1(n_e, P_m) = \frac{P_f + P_p + P_b}{J_e n_e}$,
$b_1(n_e, P_m) = \left(\frac{H_u \eta_i \sqrt{T_m/T_a} V_d}{120 J_e R T_m \lambda L_{th}}\right)(s_i P_m + y_i)$,
$f_2(n_e, P_m) = \dot{m}_{ai0} - \sqrt{\frac{T_m}{T_a}}\frac{V_d}{120RT_m}(s_i P_m + y_i)n_e$,
$b_2(n_e, P_m) = \dot{m_{ai1}}\frac{P_a}{\sqrt{T_m}}\beta_2(P_r)$.

E. Throttle Actuator Model

The DC drive dynamics [20], possesses a block structure controllable [21]:

$$\begin{aligned} \frac{d\alpha}{dt} &= \omega_a \\ \frac{d\omega_a}{dt} &= \frac{k_t i_a - T_L}{J} \\ \frac{di_a}{dt} &= \frac{-R_d i_a - \lambda_0 \omega_a + \upsilon_a}{L} \end{aligned} \tag{16}$$

where α, ω_a, i_a and υ_a are the position, speed, current and voltage, respectively,of the throttle drive, T_L is the drive load torque, J is the moment of inertia, L and R_d are the drive inductance and resistance, respectively, and k_t and λ_0 are the torque and e.m.f. constants, respectively.

F. The Complete Model (Engine and Actuator)

A block diagram of the complete closed-loop system is shown in Fig 1.

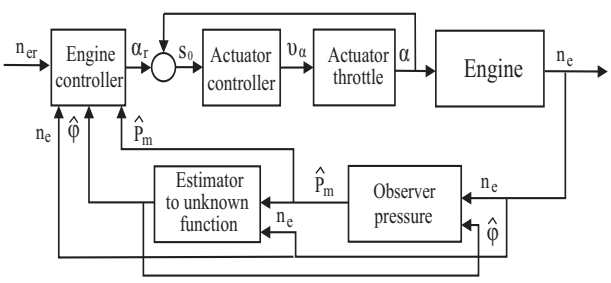

Fig. 1. BLOCK DIAGRAM OF CLOSED-LOOP SYSTEM

Now to satisfy the control objective, which is the engine speed tracking, we define the control error and new state variables as

$$x_1 = n_e - n_{er}, \;\; x_2 = P_m, \;\; x_3 = \alpha, \;\; x_4 = \omega_a, \;\; x_5 = i_a$$

where n_{er} and α_r is the engine speed and throttle position references, respectively. Then, using the engine model (15) and actuator model (16), the complete model system is presented of the form

$$\begin{aligned} \dot{x}_1 &= \bar{f}_1(x_1, \varphi) + \bar{b}_1(x_1, \varphi)x_2 \\ \dot{x}_2 &= \bar{f}_2(x_1, x_2) + \bar{b}_2(x_2)\beta_1(x_3) \\ \dot{x}_3 &= x_4 \\ \dot{x}_4 &= a_{45}x_5 - a_{40}T_L \\ \dot{x}_5 &= a_{55}x_5 - a_{54}x_4 + b_5\upsilon_a \end{aligned} \tag{17}$$

where $\bar{f}_1(x_1, \varphi) = -\frac{P_f + P_b}{J_e(x_1 + n_{er})} + \dot{n}_{er} + \varphi y_i$,
$\bar{b}_1(x_1, \varphi) = -(\frac{P_p}{J_e(x_1 + n_{er})} - \varphi s_i)$,
$\varphi = \left(\frac{H_u \eta_i \sqrt{T_m/T_a} V_d}{120 J_e R T_m \lambda L_{th}}\right)$,
$\bar{f}_2(x_1, x_2) = \frac{RT_m}{V_m}(\dot{m_{ai0}} - \sqrt{\frac{T_m}{T_a}}\frac{V_d}{120RT_m}(s_i x_2 + y_i)(x_1 + n_r))$,
$\bar{b}_2(x_2) = \frac{RT_m}{V_m}(\dot{m_{ai1}}\frac{P_a}{\sqrt{T_m}}\beta_2(x_2))$,
$a_{45} = \frac{k_t}{J}$, $a_{40} = \frac{1}{J}$, $a_{54} = \frac{\lambda_0}{L}$, $a_{55} = \frac{R}{L}$ and $b_5 = \frac{1}{L}$

III. CONTROL DESIGN

The control problem is to force the engine speed n_e to track some desired reference n_{er}. To design such controller we need to estimate certain state and unknown function of the system. In our case the unknown state is the manifold pressure x_2 and the unknown function is φ. Therefore, it is necessary to design a robust observer to estimate the manifold pressure $\hat{x}_2$ and function $\hat{\varphi}$.

A. Observer Design

Now in this subsection, we will design two observers, one to estimate the manifold pressure and another to estimate the unknown function φ, both observers will be designed by means of the sliding mode technique.

1) Manifold Pressure Observer: First, a sliding mode observer design problem for the manifold pressure x_2, is considered. To solve this problem, the following observer is proposed:

$$\begin{aligned} \dot{\hat{x}}_1 &= f_a(x_1, \hat{\varphi}) + f_b(x_1, \hat{\varphi})\hat{x}_2 + \upsilon_1 \\ \dot{\hat{x}}_2 &= \rho\bar{f}_2(x_1, \hat{x}_2) + \rho\bar{b}_2(\hat{x}_2)\beta_1(x_3) + \upsilon_2 \end{aligned} \tag{18}$$

where $\hat{x}_1$ and $\hat{x}_2$ are the estimates of crank shaft speed x_1 and manifold pressure x_2, respectively, $f_a = (P_f + P_b)/J_e x_1 + \hat{\varphi} y_i$, $f_b = (0.206x_1 - 0.969)/J_e + \hat{\varphi} s_i$, υ_1 and υ_2 are the injected observer inputs [16] selected of the form

$$\begin{aligned} \upsilon_1 &= -k_{11}[|\tilde{x}_1|^{1/2}\text{sign}(\tilde{x}_1) + \mu|\tilde{x}_1|^{3/2}\text{sign}(\tilde{x}_1)] \\ \upsilon_2 &= -k_{12}[1/2\text{sign}(\tilde{x}_1) + 2\mu\tilde{x}_1 + 3/2\mu^2|\tilde{x}_1|^2\text{sign}(\tilde{x}_1)] \end{aligned} \tag{19}$$

where $\tilde{x}_1 = x_1 - \hat{x}_1$ and $\tilde{x}_2 = x_2 - \hat{x}_2$ are the the estimation errors, $\mu \geq 0$, $k_{11} > 0$ and $k_{12} > 0$ are observer gains.

2) Adaptive Sliding Mode Observer to Estimate an Unknown Function: With the knowledge of the $\hat{x}_2$, we design an adaptive SM observer to estimate the unknown function φ; the structure of this observer is as follows:

$$\begin{aligned} \dot{\hat{\sigma}} &= f_c(x_1, \hat{x}_2) + f_d(\hat{x}_2)\hat{\varphi} + \upsilon_1 \\ \dot{\hat{\varphi}} &= \frac{\upsilon_2}{f_d(\hat{x}_2)} \end{aligned} \tag{20}$$

where $\hat{\sigma}$ and $\hat{\varphi}$ are the estimates of the crank shaft speed x_1 and unknown function φ, respectively, $f_c = (P_f + P_b) + P_b)/J_e x_1$, $f_d = y_i + s_i \hat{x}_2$, and v_1 e v_2 are the observer injected inputs [16] to be defined later. Now, we define the estimation errors as $\tilde{\sigma} = x_1 - \hat{\sigma}$ and $\tilde{\varphi} = \varphi - \hat{\varphi}$. The injection observer signals are chosen as

$$\begin{aligned} v_1 &= -k_{21}[|\tilde{\sigma}|^{1/2}\text{sign}(\tilde{\sigma}) + \mu_1|\tilde{\sigma}|^{3/2}\text{sign}(\tilde{\sigma})] \\ v_2 &= -k_{22}[1/2\text{sign}(\tilde{\sigma}) + 2\mu_1\tilde{\sigma} + 3/2\mu_1^2|\tilde{\sigma}|^2\text{sign}(\tilde{\sigma})] \end{aligned} \tag{21}$$

we defined $\mu_1 \geq 0$ as a scalar, and k_{21} e k_{22} are observer gains.

B. Engine adaptive backstepping controller design

The system (17) has the strict feedback or block controllable form, and the relative degree of the system with respect to the control error x_1 is equal to five. To solve this problem, we use the obtained estimates $\hat{x}_2$ and $\hat{\varphi}$.The combination of the backstepping technique [10], HOSM algorithm [11] and adaptive SM observer [14], [18] will be implemented in order to design, first, an adaptive sliding manifold, and then the third order SM algorithm will be implemented to make this manifold be attractive. Define $z_1 = x_1$, which is the output to be forced to zero, and setting $\tilde{x}_2 = x_2 - \hat{x}_2$, $\tilde{\varphi} = \varphi - \hat{\varphi}$, a Lyapunov function candidate is formed as

$$V_1 = \frac{1}{2}z_1^2. \tag{22}$$

The time derivative of (22) along the trajectories of (17) is calculated of the form

$$\begin{aligned} \dot{V}_1 &= z_1(\bar{f}_1(x_1, \varphi) + \bar{b}_1(x_1, \varphi)x_2) \\ &= z_1(\bar{f}_1(x_1, \hat{\varphi} + \tilde{\varphi}) + \bar{b}_1(x_1, \hat{\varphi} + \tilde{\varphi})(\hat{x}_2 + \tilde{x}_2)). \end{aligned} \tag{23}$$

The desired value x_{2r} of the virtual control x_2 in the first block of (17) is selected in order to introduce a desired dynamics $-k_1 z_1$ with $k_1 > 0$:

$$x_{2r} = \left(\frac{-k_1 z_1 - \bar{f}_1(x_1, \hat{\varphi})}{\bar{b}_1(x_1, \hat{\varphi})}\right). \tag{24}$$

Now, defining the second error

$$z_2 = \hat{x}_2 - x_{2r} \tag{25}$$

and substituting (24) in (23) yields

$$\begin{aligned} \dot{V}_1 = &-k_1 z_1^2 + \bar{b}_1(x_1, \hat{\varphi})z_2 z_1 + \bar{f}_{11}(\hat{x}_2, \tilde{x}_2)z_1\tilde{\varphi} \\ &+ \bar{b}_{11}(x_1, \tilde{\varphi})z_1\tilde{x}_2. \end{aligned} \tag{26}$$

where $\bar{f}_{11}(\hat{x}_2, \tilde{x}_2) = s_i\hat{x}_2 + s_i\tilde{x}_2 - y_i$ and $\bar{b}_{11}(x_1, \tilde{\varphi}) = \tilde{\varphi}s_i - P_p/J_e(x_1 - n_r)$.

At the second step, the following Lyapunov candidate function is formed as

$$V_2 = V_1 + \frac{1}{2}z_2^2. \tag{27}$$

Taking the time derivative of (27) results in

$$\begin{aligned} \dot{V}_2 &= \dot{V}_1 + z_2\dot{z}_2 \\ &= \dot{V}_1 + z_2(\bar{f}_2(x_1, \hat{x}_2 + \tilde{x}_2) + \bar{b}_2(\hat{x}_2 + \tilde{x}_2)v(x_3) \\ &- \dot{x}_{2r}). \end{aligned} \tag{28}$$

where $v(x_3) = \beta_1(x_3)$. To introduce the desired dynamics $-k_2 z_2$ for z_2, the desired value v_r of the virtual control $v(x_3)$ is proposed of the following form:

$$v_r = \frac{-k_2 z_2 - \bar{b}_1(x_1, \hat{\varphi})z_1 - \bar{f}_2(x_1, \hat{x}_2) + \dot{x}_{2r}}{\bar{b}_2(\hat{x}_2)} \tag{29}$$

with $k_2 > 0$, where the derivative $\dot{x}_{2r}$ can be obtained by means of a robust exact differentiator proposed in [22].

Setting

$$z_3 = v(x_3) - v_r$$

and using (29) in (28) yields

$$\begin{aligned} \dot{V}_2 &= -k_1 z_1^2 - k_2 z_2^2 + \bar{b}_2(\hat{x}_2)z_2 z_3 + \bar{f}_{21}(x_1)z_2\tilde{x}_2 \\ &+ \bar{b}_{22}(x_3)z_2\beta(\tilde{x}_2) + \bar{f}_{11}(\hat{x}_2, \tilde{x}_2)z_1\tilde{\varphi} + \bar{b}_{11}(x_1, \tilde{\varphi})z_1\tilde{x}_2. \end{aligned} \tag{30}$$

where $\bar{f}_{21}(x_1) = (R/V_m)\sqrt{T_m/T_a}(V_d/120R)(x_1 + n_r)s_i$ and $\bar{b}_{22}(x_3) = (RT_m/V_m)\dot{m}_{ai1}(P_a/T_m)v(x_3)$.

To calculate angle reference x_{3r} we put $z_3 = 0$, that means $v(x_{3r}) = v_r$, and using the expression (13), we have

$$1 - \cos(x_{3r}) - \frac{{\alpha_0}^2}{2} = v_r \tag{31}$$

Thus,the drive reference angle x_{3r} is calculated as

$$x_{3r} = cos^{-1}\left(1 - v_r - \frac{\alpha_0^2}{2}\right). \tag{32}$$

Now, the sliding function s_0 for the DC drive is formulated as

$$s_0 = x_3 - x_{3r}. \tag{33}$$

Then defining the derivatives

$$\begin{aligned} s_1 &= \dot{s}_0 \\ s_2 &= \dot{s}_1 \end{aligned} \tag{34}$$

system (17) in the new variables z_1, z_2, s_0, s_1 and s_2 can be represented of the form

$$\begin{aligned} \dot{z}_1 &= -k_1 z_1 + \bar{b}_1(x_1, \hat{\varphi})z_2 + \bar{f}_{11}(\hat{x}_2, \tilde{x}_2)\tilde{\varphi} + \bar{b}_{12}(x_2, \tilde{\varphi})\tilde{x}_2 \\ \dot{z}_2 &= -\bar{b}_1(x_1, \hat{\varphi})z_1 - k_2 z_2 + \bar{b}_2(\hat{x}_2)s_0 + \bar{f}_{21}(x_1)\tilde{x}_2 \\ &+ \bar{b}_{22}(x_3)\beta_2(\tilde{x}_2) \\ \dot{s}_0 &= s_1 \\ \dot{s}_1 &= s_2 \\ \dot{s}_2 &= f_s(x_1, x_2, x_3, x_4, x_5) - b_s u \end{aligned} \tag{35}$$

where f_s is a continuous functions bounded in a admissible region Ω by

$$|f_s(x_1, x_2, x_3, x_4, x_5)| \leq \gamma_0 < \infty \tag{36}$$

and $b_s = a_{45}b_5$.

C. Actuator HOSM controller design

To enforce sliding mode motion on $s_0 = 0$, $s_1 = 0$ and $s_2 = 0$, we apply the following third-order sliding mode algorithm:

$$\begin{aligned} u &= -u_0 \text{sign}[\psi_{2,3}(s_0, s_1, s_2)], \quad u_0, \beta_1, \beta_2 > 0 \\ \psi_{2,3}(s_0, s_1, s_2) &= s_2 + \beta_2 \left(|s_1|^3 + |s_0|\right)^{1/6} \\ &\quad \times \text{sign}\left(s_1 + \beta_1 |s_0|^{2/3} \text{sign}(s_0)\right) \end{aligned} \tag{37}$$

where u_0,β_1 and β_2 are the control gains. The implementation of the proposed third-order SM controller requires the calculation of the derivatives s_1 and s_2. To obtain these derivatives, a sliding mode exact robust differentiator [11] can be employed. We use the second-order robust exact differentiator defined by

$$\begin{aligned} \dot{\xi}_0 &= \gamma_0 \quad \gamma_0 = -\delta_0 |\xi_0 - s_0|^{2/3} \text{sign}(\xi_0 - s_0) + \xi_1 \\ \dot{\xi}_1 &= \gamma_1 \quad \gamma_1 = -\delta_1 |\xi_1 - \gamma_0|^{1/2} \text{sign}(\xi_1 - \gamma_0) + \xi_2 \\ \dot{\xi}_2 &= -\delta_2 \text{sign}(\xi_2 - \gamma_1) \end{aligned} \tag{38}$$

where ξ_0, ξ_1 and ξ_2 are the estimates of the sliding variable s_0 and its derivatives s_1 and s_2, respectively, and δ_i, $i = 0, 1, 2$, are the differentiator gains.

The complete closed-loop system in new variables is shown as follows

$$\begin{cases} \dot{z}_1 &= -k_1 z_1 + \bar{b}_1(x_1, \hat{\varphi}) z_2 + \bar{f}_{11}(\hat{x}_2, \tilde{x}_2)\tilde{\varphi} + \bar{b}_{12}(x_2, \tilde{\varphi})\tilde{x}_2 \\ \dot{z}_2 &= -\bar{b}_1(x_1, \hat{\varphi}) z_1 - k_2 z_2 + \bar{b}_2(\hat{x}_2) s_0 + \bar{f}_{21}(x_1)\tilde{x}_2 \\ &\quad + \bar{b}_{22}(x_3)\beta_2(\tilde{x}_2) \end{cases} \tag{39}$$

$$\begin{cases} \dot{s}_0 &= s_1 \\ \dot{s}_1 &= s_2 \\ \dot{s}_2 &= f_s(x_1, x_2, x_3, x_4, x_5) - b_s(u_0 \\ &\quad \text{sign}\left[\psi_{2,3}(s_0, s_1, s_2)\right]) \end{cases} \tag{40}$$

$$\begin{cases} \dot{\xi}_0 &= \gamma_0 \quad \gamma_0 = -\delta_0 |\xi_0 - s_0|^{2/3} \text{sign}(\xi_0 - s_0) + \xi_1 \\ \dot{\xi}_1 &= \gamma_1 \quad \gamma_1 = -\delta_1 |\xi_1 - \gamma_0|^{1/2} \text{sign}(\xi_1 - \gamma_0) + \xi_2 \\ \dot{\xi}_2 &= -\delta_2 \text{sign}(\xi_2 - \gamma_1) \end{cases} \tag{41}$$

$$\begin{cases} \dot{\tilde{x}}_1 &= f_b(x_1, \hat{\varphi})\tilde{x}_2 - k_{11}[|\tilde{x}_1|^{1/2} \text{sign}(\tilde{x}_1) \\ &\quad + \mu |\tilde{x}_1|^{3/2} \text{sign}(\tilde{x}_1)] \\ \dot{\tilde{x}}_2 &= \bar{f}_2(x_1, x_2 - \hat{x}_2) + \bar{b}_2(x_2 - \hat{x}_2)\beta_1(x_3) \\ &\quad - k_{12}[1/2 \text{sign}(\tilde{x}_1) + 2\mu \tilde{x}_1 + 3/2\mu^2 |\tilde{x}_1|^2 \text{sign}(\tilde{x}_1)] \\ \dot{\tilde{\sigma}} &= f_d(\hat{x}_2)\tilde{\varphi} - k_{21}[|\tilde{\sigma}|^{1/2} \text{sign}(\tilde{\sigma}) + \mu_1 |\tilde{\sigma}|^{3/2} \text{sign}(\tilde{\sigma})] \\ \dot{\tilde{\varphi}} &= -\left(\frac{1}{f_d(\hat{x}_2)}\right) k_{22}[1/2 \text{sign}(\tilde{\sigma}) + 2\mu_1 \tilde{\sigma} \\ &\quad + 3/2\mu_1^2 |\tilde{\sigma}|^2 \text{sign}(\tilde{\sigma})] + f_e \end{cases} \tag{42}$$

The stability of closed loop system (39)-(42) is outlined in the stepwise procedure:

Step A) Reaching phase of the projection motion (42).

Step B) The SM robust exact differentiator stability of the projection motion (41).

Step C) The HOSM stability of the projection motion (40).

Step D) The SM motion stability of (39) on the manifold $\tilde{x}_2 = \tilde{\varphi} = s_0 = 0$ and in the vicinity of $z_1 = 0$.

Step A) Introducing the transformation

$$q = f_d(\hat{x}_2)\tilde{\varphi} \quad \text{and} \quad w = f_b(x_1, \hat{\varphi})\tilde{x}_2 \tag{43}$$

the subsystem (42) reduces to

$$\begin{aligned} \dot{\tilde{x}}_1 &= w - k_{11}[|\tilde{x}_1|^{1/2} \text{sign}(\tilde{x}_1) + \mu_1 |\tilde{x}_1|^{3/2} \text{sign}(\tilde{x}_1)] \\ \dot{w} &= \dot{f}_b(x_1)\tilde{x}_2 + f_b(x_1)\chi - k_{12}[1/2 \text{sign}(\tilde{x}_1) + 2\mu_1 \tilde{x}_1 \\ &\quad + 3/2\mu_1^2 |\tilde{x}_1|^2 \text{sign}(\tilde{x}_1)] \\ \dot{\tilde{\sigma}} &= q - k_{21}[|\tilde{\sigma}|^{1/2} \text{sign}(\tilde{\sigma}) + \mu_1 |\tilde{\sigma}|^{3/2} \text{sign}(\tilde{\sigma})] \\ \dot{q} &= \dot{f}_d(\hat{x}_2)\tilde{\varphi} + f_e f_d(\hat{x}_2) - k_{22}[1/2 \text{sign}(\tilde{\sigma}) + 2\mu_1 \tilde{\sigma} \\ &\quad + 3/2\mu_1^2 |\tilde{\sigma}|^2 \text{sign}(\tilde{\sigma})] \end{aligned} \tag{44}$$

where $\chi = \bar{f}_2(x_1, x_2 - \hat{x}_2) + [\bar{b}_2(x_2 - \hat{x}_2)]u(x_3)$, and we assume that the following inequalities

$$\begin{aligned} |\dot{f}_b(x_1)\tilde{x}_2 + f_b(x_1)\chi| &\leq C > 0 \\ |\dot{f}_d(\hat{x}_2)\tilde{\varphi} + f_e f_d(\hat{x}_2)| &\leq L > 0 \end{aligned} \tag{45}$$

are satisfied in an admissible region Ω_0. Then, there are k_{11}, k_{12}, k_{21} and k_{22} such that the system (42) is finite time globally stable [16], i.e., its solution converges in finite time to the origin $(\tilde{x}_1, w) = (\tilde{x}_1, \tilde{x}_2) = (\tilde{\sigma}, q) = (\tilde{\sigma}, \tilde{\varphi}) = (0, 0)$.

Step B) To analyze the stability of the robust differentiator (41), we rely on [11], where it was shown that there exist $\delta_i > 0$, $i = 0, 1, 2$, such that the estimates $\xi_0(t)$, $\xi_1(t)$ and $\xi_2(t)$ converge to the real variables $s_0(t)$, $s_1(t)$ and $s_2(t)$ in finite time. These estimates are then implemented in controller (37) instead of the real variables.

Step C) The stability analysis of the projection motion (40) is based on [11], where it was shown that there exits a set of constants $u_0 > 0$, $\beta_1 > 0$, and $\beta_2 > 0$ such that the state vector of the closed-loop sub system (40) converges in finite time to the third-order SM set

$$s_0 = 0 \qquad s_1 = 0 \qquad s_2 = 0 \tag{46}$$

Step D) The motion on the sliding manifold (46) is defined by (39) constrained to $\tilde{x}_2 = \tilde{\varphi} = s_0 = 0$:

$$\begin{aligned} \dot{z}_1 &= -k_1 z_1 + \bar{b}_1(x_1, \hat{\varphi}) z_2 \\ \dot{z}_2 &= -\bar{b}_1(x_1, \hat{\varphi}) z_1 - k_2 z_2. \end{aligned} \tag{47}$$

And the Lyapunov function derivative $\dot{V}_2$ (30) reduces to

$$\dot{V}_2 = -k_1 z_1^2 - k_2 z_2^2 < 0. \tag{48}$$

If we select the control gains as $k_1 > 0$ and $k_2 > 0$, then the system (47) will be asymptotically stable, that is the control errors $z_1(t)$ and $z_2(t)$ tends to zero as $t \to \infty$.

IV. SIMULATIONS

In this Section, we verify the performance of the proposed control scheme by means of numeric simulations.

We consider a MVEMs with the following nominal parameters: $V_d = 1.275\ L$, $R = 0.00287$, $V_m = 0.0017$, $I = 480(2\pi/60)^2$, $H_u = 4300$, $L_{th} = 14.67$, $\lambda = 1.0$, $T_m = 293$, $T_a = 293$, $, P_c = 0.4125$, $P_a = 1.013$, $P_r = P_m/P_a$, $\dot{m}_{ai0} = 5.9403$, $\dot{m}_{ai1} = 0$, $si = 0.961$, $yi = -0.07$. The velocity reference signal increases from 0 to 3 krpm in the first 8 s and then, it remains constant for 8 to 15 s, again increases from 3 krpm to 4 krpm it remains constant for 15 to 20 s, and finally constant in 4 krpm it remains constant for 20 to 30 s. In figure 2 shows the output tracking result of the engine velocity, in figure 3 is presented the response of the output tracking of the estimation of the pressure in manifold, and finally the behavior of estimation of the unknown function is shown in figure 4.

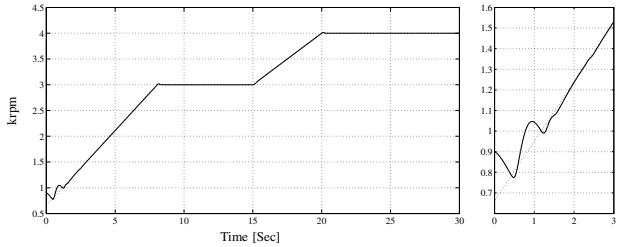

Fig. 2. VELOCITY ENGINE n_e (SOLID) AND REFERENCE n_{er} (DASHED).

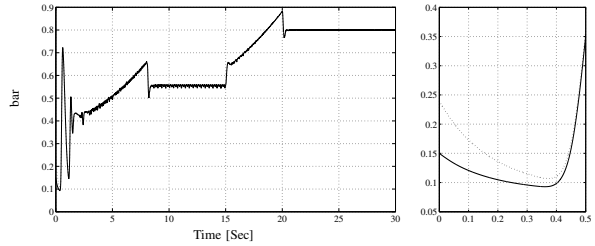

Fig. 3. PRESSURE IN MANIFOLD P_m (DASHED) AND ITS ESTIMATION $\hat{P}_m$ (SOLID).

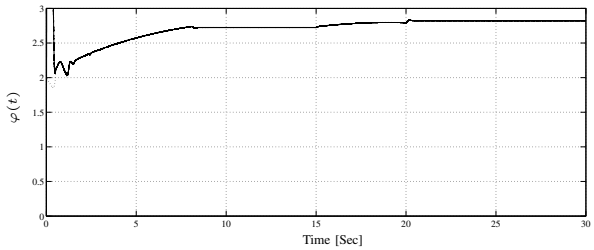

Fig. 4. UNKNOWN FUNCTION φ (DASHED) AND ITS ESTIMATION $\hat{\varphi}$ (SOLID).

V. CONCLUSIONS

A SM controller with adaptive observer for internal combustion engine, is designed. The control design was based on the combination of the backstepping, HOSM control and SM observer design techniques. The proposed observers provide the satisfactory estimation of the unmeasured manifold pressure and the unknown plant parameters function. To design both of them, the High Order Sliding Mode algorithms are implemented. In particular, this control technique is applied to ensure the finite time convergence and robustness. This fact is verified by numerical simulations.

REFERENCES

[1] A. G. Loukianov, S. Dodds, W. Hosny, and J. Vittek, "A robust automotive controller design," in *Control Applications, 1997., Proceedings of the 1997 IEEE International Conference on*, 1997, pp. 806–811.

[2] J. J. Moskwa and J. Hedrick, "Automotive engine modeling for real time control application," in *American Control Conference*, 1987, pp. 341–346.

[3] L. Guzzella and C. Onder, *Introduction to Modeling and Control of Internal Combustion Engine Systems*. Springer, 2009.

[4] Q. Ahmed and A. Bhatti, "Second order sliding mode observer for estimation of si engine volumetric efficiency amp; throttle discharge coefficient," in *Variable Structure Systems (VSS), 2010 11th International Workshop on*, 2010, pp. 307–312.

[5] E. Hendricks and S. Sorenson, "Mean value si engine model for control studies," in *American Control Conference, 1990*, 1990, pp. 1882–1887.

[6] E. Hendricks and T. Vesterholm, "The analysis of mean value si engine models," in *SAE Technical Paper*, 1992.

[7] E. Hendricks and S. Sorenson, "Mean value modelling of spark ignition engines," in *SAE Technical Paper*, no. 900616, 1990.

[8] E. Hendricks, "Mean value modelling of large turbocharged two-stroke diesel engines," in *SAE Technical Paper*, 1989.

[9] R. Rajamani, *Vehicle Dynamics and Control*, ser. Mechanical Engineering. Springer, 2012.

[10] M. Krstić, I. Kanellakopoulos, and P. Kokotović, *Nonlinear and adaptive control design*, ser. Adaptive and learning systems for signal processing, communications, and control. Wiley, 1995.

[11] A. Levant, "Higher-order sliding modes, differentiation and output-feedback control," *International Journal of Control*, vol. 76, pp. 924–941, 2003.

[12] S. V. Drakunov and V. I. Utkin, "Sliding mode control in dynamic systems," *International Journal of Control*, vol. 55, pp. 1029–1037, 1992.

[13] V. Utkin, J. Guldner, and J. Shi, *Sliding mode control in electromechanical systems*, E. rogers and J. O´Reilly, Eds. CRC Press, 1999.

[14] S. Drakunov, "Sliding-mode observers based on equivalent control method," in *Decision and Control, 1992., Proceedings of the 31st IEEE Conference on*, 1992, pp. 2368–2369 vol.2.

[15] S. V. Drakunov and V. A. Utkin, "Sliding mode observers. tutorial," in *Decision and Control, 1995., Proceedings of the 34th IEEE Conferenceon*, vol. 4, Dec. 1995, pp. 3376–3378 vol.4.

[16] E. Cruz-Zavala, J. Moreno, and L. Fridman, "Uniform robust exact differentiator," in *Decision and Control (CDC), 2010 49th IEEE Conference on*, 2010, pp. 102–107.

[17] A. Levant, "Sliding order and sliding accuracy in sliding mode control," *International Journal of Control*, vol. 58, no. 6, pp. 1247–1263, 1993.

[18] J. Davila, L. Fridman, and A. Levant, "Second-order sliding-mode observer for mechanical systems," *Automatic Control, IEEE Transactions on*, vol. 50, no. 11, pp. 1785–1789, 2005.

[19] E. Hendricks, A. Chevalier, M. Jensen, and S.Sorenson, "Modelling of the intake manifold filling dynamics," in *SAE Technical Paper*, 1996.

[20] I. Gottlieb, *Electric Motors and Control Techniques*. McGraw-Hill Education, 1994. [Online]. Available: http://books.google.com.mx/books?id=99xxCjXFbnEC

[21] A. Loukianov, "Nonlinear block control with sliding mode," *Automation and Remote Control*, vol. 59, no. 7, pp. 916–933, 1998.

[22] A. Levant, "Robust exact differentiation via sliding mode technique," *Automatica*, vol. 34, pp. 379 – 384, 1998.